Sorption, Diffusion, and Pervaporation Separation of Water–Acetic Acid Mixtures Through the Blend Membranes of Sodium Alginate and Guar Gum-Grafted-Polyacrylamide

UDAYA S. TOTI, MAHADEVAPPA Y. KARIDURAGANAVAR, KUMARESH S. SOPPIMATH, TEJRAJ M. AMINABHAVI

Department of Chemistry, Polymer Research Group, Karnatak University, Dharwad 580 003, India

Received 24 December 2000; accepted 3 February 2001

ABSTRACT: Nonporous homogeneous dense membranes were prepared from the blends of sodium alginate (Na–Alg) with guar gum-grafted polyacrylamide (GG-*g*-PAAm) in the ratios of 3 : 1 and 1 : 1 and these were tested for the pervaporation separation of water–acetic acid mixtures at 30°C. Blend compatibility was studied in solution by measuring the viscosity and the speed of sound. Membranes were crosslinked by glutaraldehyde. The GG-*g*-PAAm polymer and the crosslinked blend membranes were characterized by Fourier transform infrared spectra. High separation selectivity was exhibited by the pure Na–Alg membrane for water–acetic acid (HAc) mixtures containing 20 mass % of water. The permeation flux increased with increasing mass percent of water in the feed as well as with an increase in the amount of GG-*g*-PAAm in the blend, but separation selectivity decreased. Sorption selectivity was higher for the Na–Alg membrane than for the blend membranes, but it decreased with increasing mass percent of GG-*g*-PAAm in the blends. Diffusion selectivity values vary systematically with the blend composition, but not with the amount of water in the feed. Diffusion coefficients of the water–HAc mixtures were calculated from Fick's equation using sorption data and compared with those calculated from flux values obtained in pervaporation experiments. The Arrhenius activation parameters were calculated for the 20 mass % of water in the feed using flux and diffusion data obtained at 30, 40, and 50°C. The diffusion and pervaporation results are explained in terms of solution–diffusion concepts. © 2002 John Wiley & Sons, Inc. J Appl Polym Sci 83: 259–272, 2002

Key words: pervaporation; acetic acid–water mixtures; sodium alginate; guar gum; blend membranes

INTRODUCTION

Pervaporation (PV) is a membrane-based separation technique used to separate azeotropic liquid mixtures.[1] In this technique, the feed mixture is kept in contact with one side of the nonporous polymer membrane while the permeate is removed in a vapor state from the opposite side under the influence of a continuous vacuum. This happens due to the molecular transport of liquid across the swollen membrane, which acts as a thin extracting solvent layer. The solvent molecules are continuously removed at the downstream side in the vapor form; these are evaporated and then condensed as liquids. It is thus

Correspondence to: T. M. Aminabhavi (aminabhavi@yahoo.com; cc to rrist@sancharnet.in; rrist@bgl.vsnl.net.in).

Contract grant sponsor: Department of Science and Technology, New Delhi; contract grant number: SP/S1/H-26/96 (PRU).

Journal of Applied Polymer Science, Vol. 83, 259–272 (2002)

necessary to bring into the system a quantity of energy, which is at least equal to the heat of evaporation. Contrary to other membrane processes, PV requires sorption, permeation, and vaporization of a part of the liquid through the membrane. Therefore, PV can be effective only when selectivity of the migrating liquid is much higher than is the vaporization. An important feature of the PV process is that the membrane must exhibit strong preferential interactions with one of the solvents.

In recent years, there is a growing interest to use the grafted,[2] composite,[3] or blend[4] membranes in the PV separation of aqueous–organic mixtures. In our earlier study,[2] we used poly(vinyl alcohol)-grafted acrylamide membranes having different grafting ratios for the separation of water–acetic acid (HAc) mixtures. In continuation of this research, we now report the synthesis of new blend membranes of two natural polymers, namely, sodium alginate (Na–Alg) and guar gum (GG), with a synthetic polyacrylamide (PAAm). GG by itself does not have film-forming properties, but Na–Alg can form stable films.[5] The GG-grafted PAAm (GG-*g*-PAAm) was blended with Na–Alg in different ratios to produce the nonporous homogeneous dense membranes. The polymers were characterized by FTIR, and the blend compatibility was studied by measuring the viscosity and the speed of sound in solution. Thin membranes ($\cong$30 μm) were fabricated and used in the PV separation of water–HAc mixtures.

An HAc and water mixture is particularly chosen because of its importance in chemical industries. HAc is used in the synthesis of vinyl acetate, terephthalic acid, cellulose esters, and esters.[6] Even though HAc and water do not form azeotropic mixtures, their separation by simple distillation is not feasible due to their close relative volatility. In the earlier literature, several membranes were used[7–17] to separate water–HAc mixtures, but the blend membranes of the type developed here have not been used. PV experiments were performed at 30°C. Dynamic sorption experiments were also performed at 30°C for 10, 20, and 30 mass % of water in the feed mixture. Diffusion coefficients were calculated both from the sorption and PV experiments. These results are discussed in terms of separation selectivity and flux. Diffusion data were compared with those obtained from the sorption experiments. It was found that the pure Na–Alg membrane gave the best selectivity to water when tested for a 20 mass % water-containing mixture, but the membrane selectivity decreased with an increasing amount of GG-*g*-PAAm in the blend. The flux values increased with an increasing amount of GG-*g*-PAAm in the blend and the blend membranes containing more than 50 mass % of GG-*g*-PAAm were not stable for the PV experiments, probably due to an increase in polymer crystallinity.

EXPERIMENTAL

Materials

Sodium alginate was purchased from Luba Chemicals (Mumbai, India). GG was purchased from S.D. Fine Chemicals (Mumbai, India). GG-grafted acrylamide was prepared as per the procedure given earlier.[18] Ceric ammonium nitrate (CAN), HAc, and methanol were of AR-grade samples, which were obtained from S.D. Fine Chemicals; these were used as received. Double-distilled water was used throughout the research.

Synthesis of Graft Copolymer

GG-*g*-PAAm was synthesized by reacting GG with acrylamide at 60°C using CAN as an initiator.[18] In brief, a 2% aqueous GG solution was prepared and stirred well for 1 h with 0.105 mol of acrylamide at 60°C. The initiator solution containing 5.47×10^{-4} mol of CAN was added to the mixture and stirred well for another 5 h. The mass obtained was precipitated in acetone and washed with a 7 : 3 ratio of a water : methanol mixture to remove the homopolymer formed. Then, the solid mass was dried in an electrically controlled oven at 40°C and weighed.

Fourier Transform Infrared (FTIR) Spectroscopy

The grafting reaction was confirmed by FTIR (Nicolet, Model Impact 410, USA). Polymer samples were crushed to make KBr pellets under a hydraulic pressure of 600 kg and spectra were taken in the wavelength range of 400–4000 cm^{-1}.

Blend-compatibility Study

Blend compatibility was studied at 30°C from the viscosity data and by plotting the reduced viscosity (η_{sp}/c) and adiabatic compressibility (β_{ad}) of the polymer solutions versus the blend composition. The viscosity was measured on 0.5% (w/v) of the aqueous solutions of Na–Alg, GG-*g*-PAAm,

and their blend mixtures in the selected compositions of 20/80, 40/60, 60/40, and 80/20 using the Schott–Gerate viscometer (Model AVS 350, Germany).[19]

The speed of sound (u) and density (ρ) of the polymer solutions were used to calculate the adiabatic compressibility (β_{ad}). The speed of sound values were measured using a variable path single-crystal interferometer (Mittal Enterprises, Model M-84, New Delhi, India) as described earlier.[20] An interferometer was used at a frequency of 1 kHz, and the instrument was calibrated using water and benzene. The measured speed of sound values were accurate to ± 2 ms^{-1}. The densities of the pure polymer solutions and their blends were measured using a pycnometer having a bulb volume of 10 cm^3 and a capillary bore with an internal diameter of 1 mm.[21]

Membrane Preparation

The 4 mass % stock solution of Na–Alg was prepared in water. The stock solution, 100 mL, was taken in a beaker and mixed with 0.00175 mol of GA (0.1 mL of 25 wt % in water). This mixture was stirred for 2 h at 25°C and poured uniformly on a glass plate. Membranes were dried at room temperature for nearly 2–3 days. The cast membranes were crosslinked by immersing in a 1% HCl solution taken in an equimolar mixture of methanol and water for 24 h, then washed thoroughly in water and dried. The Na–Alg membrane thus prepared is designated as M-1.

To prepare the blend membranes, 4 mass % of the stock solutions of Na–Alg and GG-*g*-PAAm were mixed in the ratio 75 : 25 (designated as M-2) and 50 : 50 (designated as M-3) at 60°C for 4 h and the solution was cooled to room temperature. To this, 0.00175 mol of GA (0.1 mL of 25 wt % in water) was added and the mixture was stirred for another 2 h. This mixture was poured onto a glass plate and the crosslinked blend membranes were prepared as described above.

Sorption Experiments

Dynamic and equilibrium sorption experiments were performed in water–HAc mixtures at 30 $\pm$ 0.5°C using an electronically controlled oven (WTB Binder, Germany). Circularly cut ($\approx$ 2.00 cm) disk-shaped membranes were kept in a vacuum oven at 25°C for 48 h before use. The initial mass of these membranes was measured on a top-loading single-pan digital microbalance (Model AE 240, Switzerland) sensitive to $\pm$0.01 mg. Samples were placed inside screw-tight test bottles containing different mixtures of water and HAc. The test bottles were then placed inside the oven maintained at 30°C. The mass measurements were done at the suitably selected time intervals by removing the samples from the test bottles, wiping the surface-adhered solvent drops by pressing the samples in between filter paper wraps, then weighing them immediately and placing them back into the oven. This step was completed within 15–20 s to minimize errors due to evaporation losses.

From the gravimetric data, percent mass uptake (M_t), equilibrium percent mass uptake (M_∞ or S), degree of swelling (DS), and diffusion coefficients (D) were calculated, respectively, using eqs. (1), (2), (3), and (4):

$$M_t = \frac{W_t - W_0}{W_0} \times 100 \tag{1}$$

$$M_\infty = \frac{W_\infty - W_0}{W_0} \times 100 \tag{2}$$

$$DS = \frac{M_\infty}{M_i} \tag{3}$$

$$\frac{M_t}{M_\infty} = \frac{4}{h}\left[\frac{Dt}{\pi}\right]^{1/2} \tag{4}$$

In the above equations, W_0 is the initial dry mass of the polymer sample; W_t and W_∞, respectively, the mass at time, t, and equilibrium mass of the membrane during sorption experiments; and h, the thickness of the membrane. The diffusion coefficients were calculated as per the published procedures.[22] The results of S, DS, and D are presented in Table I.

Sorption Selectivity (α_{sorp})

Completely equilibrated membranes with different mass percent of water containing water + HAc mixtures were removed from the test bottles, blotted to remove the surface-adhered liquid drops, and then placed back into the glass trap connected to another trap surrounded by liquid nitrogen and heated to 120°C (close to the boiling point of HAc, i.e., 117.5°C) and the vapor condensed in the cold trap, surrounded by a liquid nitrogen jar. Composition of the condensed liquid mixture was then calculated by measuring the

Table I Degree of Swelling (*DS*), Equilibrium Percent Mass Uptake (*S*), and Diffusion Coefficient (*D*)

Mass % of Water in the Feed	*DS* (kg/kg) Eq. (3)			*S* (kg/kg) Eq. (2)			*D* (m^2/s) × 10^{13} Eq. (4)		
	M-1	M-2	M-3	M-1	M-2	M-3	M-1	M-2	M-3
10	1.24	1.26	1.73	24.0	26.0	72.9	1.49	1.62	1.77
20	1.24	1.42	2.03	24.2	41.9	103	4.89	5.80	5.62
30	1.25	1.53	2.10	23.2	56.3	112	9.03	59.1	111.0
40	1.32	1.67	2.29	32.0	72.6	128	[a]	[a]	[a]
50	1.51	1.85	2.30	50.5	91.5	133			
60	1.67	2.02	2.44	66.7	101	144			
70	1.74	1.99	2.44	73.9	102	144			
80	1.74	1.98	2.45	74.4	102	144			
90	1.78	1.97	2.44	78.4	104	145			

[a] Since the diffusion process becomes very fast, the data at higher composition of water were not obtained.

refractive index (±0.0002) using an Abbe refractometer (Atago 3T, Japan). The sorption selectivity was calculated as

$$\alpha_{\text{sorp}} = \frac{M_W/M_{\text{HAc}}}{F_W/F_{\text{HAc}}} \tag{5}$$

where M_W, M_{HAc} and F_W, F_{HAc} are the mass percent of water and HAc in the membrane and feed, respectively.

PV Experiments

PV experiments were performed using the cell designed indigenously.[2] The effective surface area of the membrane in contact with the feed mixture was 32.4 cm^2 and the capacity of the PV cell was about 250 cm^3. The mass percent water in its HAc mixture was varied from 10 to 80. After taking 25 mL of the mixture in the feed compartment, the test membrane was allowed to equilibrate for 2 h. The downstream side was continuously evacuated using a vacuum pump (Toshniwal, India) at a vacuum pressure of 10 Torr. The permeate mixture was condensed in the liquid nitrogen traps. The mass of the permeate mixture collected in the trap was taken and its composition was determined by measuring its refractive index and by comparing it with a standard graph. The depleted solvent mixture of the feed component was continuously enriched with the fresh solvent mixture.

From the PV data, membrane performance was studied by calculating the total flux, J_p, separation selectivity, α_{sep}, pervaporation separation index, *PSI*, and enrichment factor, β, using the following relations:

$$J_p = \frac{W_p}{At} \tag{6}$$

$$\alpha_{\text{sep}} = \frac{P_W/P_{\text{HAc}}}{F_W/F_{\text{HAc}}} \tag{7}$$

$$PSI = J_p(\alpha_{\text{sep}} - 1) \tag{8}$$

$$\beta = \frac{C_A^P}{C_A^F} \tag{9}$$

Here, W_p is mass of the permeate; A, the area of the membrane in contact with the feed mixture; and t, the time; P_{W} and P_{HAc} are the mass percent of water and HAc respectively, in the permeate; F_{W} and F_{HAc}, the mass percent of water and HAc in the feed, respectively; and C_A^P and C_A^F, the concentrations of the permeate and the feed, respectively. The pervaporation flux and α_{sep} data are presented in Tables II and III.

RESULTS AND DISCUSSION

Synthesis and Characterization

The graft copolymerization of GG with acrylamide was attempted by a Ce(IV)-catalyzed free-radical reaction. The chelate complex formed between the —OH group of GG decomposes to generate the free-radical site. Then, grafting occurs at the active site on the backbone of GG with the

Table II Total PV Flux and Separation Selectivity Data at Different Mass Percent of Water in the Feed

Mass % of Water in the Feed	$J_p \times 10^2$ (kg m^{-2} h^{-1}) Eq. (6)			α_{sep} Eq. (7)		
	M-1	M-2	M-3	M-1	M-2	M-3
10	2.48	1.93	3.55	13.6	15.3	7.82
20	4.69	5.40	8.00	22.5	14.1	7.42
30	6.69	14.5	14.4	15.0	7.28	4.53
40	8.87	14.4	16.5	9.40	5.95	5.02
50	10.6	16.9	37.9	7.00	5.77	5.45
60	20.1	33.9	50.1	5.99	6.70	7.18
70	25.3	35.5	59.8	7.03	6.99	6.71
80	25.9	38.5	59.7	7.44	7.55	6.89

acrylamide monomer. Taking only a 0.1*M* concentration of the monomer minimizes the formation of the acrylamide homopolymer. Owen and Shen[23] reported that, as the concentration of a monomer is increased beyond 2.0*M,* it is likely that a homopolymer will be formed. With this, the grafting ratio was 365 with 98% conversion of acrylamide to give the GG-*g*-PAAm copolymer, indicating that grafting was almost successful. See the reaction scheme presented in Figure 1.

FTIR spectra of (A) GG-*g*-PAAm and (B) the M-3 membrane are presented in Figure 2. A characteristic strong and broad band appearing at $\sim$ 3357 cm^{-1} corresponds to the O—H stretching of GG, which is not involved in the grafting reaction. The characteristic peak observed at 1665 cm^{-1} corresponding to the AAm moiety confirms the grafting reaction of AAm onto the GG backbone. A shoulder band observed at 3191 cm^{-1} corresponds to N—H stretching of the primary amide, which further supports the grafting of AAm onto the GG backbone. Absorption bands observed between 1000 and 1100 cm^{-1} in the spectra of all three polymers are due to the presence of the acetyl carbonyl group of the polymer. However, an intense peak observed around this range in the spectra of M-3 indicates the crosslinking reaction.

The solution blend compatibility was confirmed using viscosity and speed of sound data. From the results of the speed of sound, adiabatic compressibility values were calculated as

$$\beta_{ad} = 1/u^2\rho \tag{10}$$

From the viscosity data, the reduced viscosity was calculated. The reduced viscosity results as well as the adiabatic compressibility data are plotted as a function of the blend composition in Figure 3. The linearity observed in these plots further support the blend compatibility in solution.[24]

Membrane Crosslinking

Effective crosslinking of the Na–Alg membrane was achieved by using 5 vol % of GA in 0.05 vol % of HCl in acetone.[25] Since our aim was to study the effect of the GG-*g*-PAAm matrix on the overall performance of the blend membrane, we prepared the loosely crosslinked matrix using a small amount of GA. If a large amount of GA is present

Table III PV Flux and Separation Selectivity at Different Temperatures for 20 Mass % of Water in the Feed Mixtures

Temperature (°C)	$J_p \times 10^2$ (kg m^{-2} h^{-1})			α_{sep}		
	M-1	M-2	M-3	M-1	M-2	M-3
30	4.69	5.40	8.00	22.05	14.13	7.42
40	7.46	7.62	9.47	18.22	10.03	4.51
50	9.61	10.5	12.87	17.62	9.67	4.33

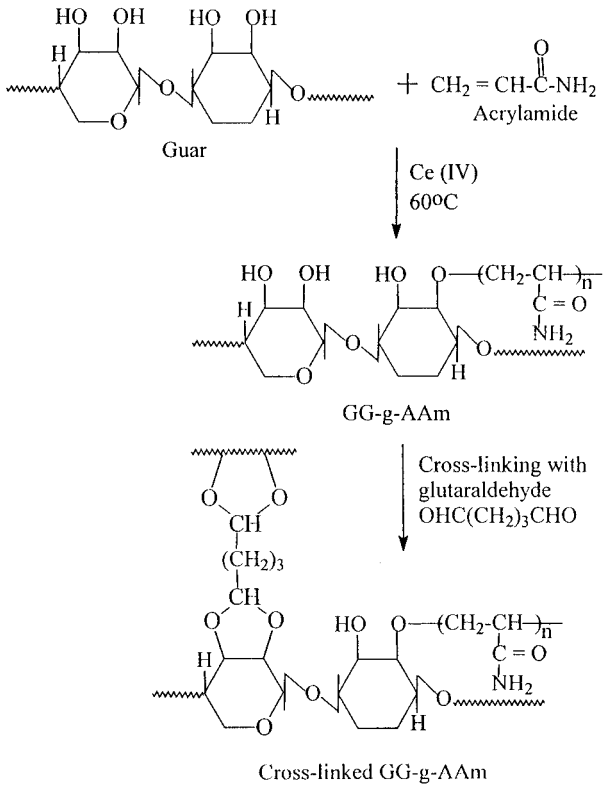

Figure 1 Grafting reaction of acrylamide onto GG.

in the final membrane, it is likely to affect the separation selectivity, probably due to the affinity of GA toward organics. During crosslinking, the presence of HCl converts the Na–Alg into the water-insoluble alginic acid, giving mechanical strength to the membrane formed.

Molecular Transport and Sorption Selectivity

When liquids permeate through the swollen polymeric membrane, there will be a coupling of fluxes leading to the permeation, which, in turn, affects the membrane performance. When polymers are used below their glass transition temperatures, thermal motion of the chain segments will be restricted, and whenever the polymer comes in contact with low molecular weight components, their interaction will increase and, thus, the chain mobility will also increase. For the binary probe mixtures under study, both components will exert an effect on the polymer chain segmental motion. The PV process may be understood in terms of the molecular transport of liquids through the barrier membranes and, thus, the phenomenon can be described by a coupling phenomenon based on the diffusion–sorption model.[26] Although numerous theories have been proposed, none of them are completely satisfactory in explaining the molecular transport of polar liquids/or their mixtures through membrane polymers containing hydrophilic groups.[27] From Table I, it is found that the degree of swelling, equilibrium percent mass uptake of the membranes, and diffusion coefficients increase with increasing water content in the feed mixture. However, due to the experimental difficulties, diffusion coefficients were calculated only up to 30 mass % of water in the binary mixture.

Figure 4 displays the dependence of mass percent uptake on the square root of time for all the three membranes in the presence of 10, 20, 30, and 40 mass % of water-containing feed mixtures at 30°C. It is observed that, with an increasing amount of water in the feed mixture, sorption also increases, indicating increased hydrophilic interactions between the water molecules and the membrane. In general, the mass percent uptake by the sodium alginate membrane (M-1) is considerably smaller than that by the blend membranes (M-2 or M-3). With an increasing amount of GG-*g*-PAAm in the blend membranes from 25% (M-2) to 50% (M-3), the mass percent uptake also increases. This suggests an increased hydrophilicity of the blend membranes at a higher amount of GG-*g*-PAAm in the blend. Shapes of the curves also vary depending upon the nature of the penetrant mixture. For instance, with the feed mixture containing 10 mass % of water, the increase in uptake of the Na–Alg membrane is much slower than that of the M-2 and M-3 membranes. However, with 20 mass % water in water + HAc mixture, the increase in uptake for the M-3 membrane is quite dramatic when compared to both the M-1 and M-2 membranes. Also, diffusion follows the non-Fickian trend since the sigmoidal trends are observed at higher amounts of GG-*g*-PAAm in the blend membrane (M-3). When 30 or 40 mass % of the water-containing mixture was used, we noticed considerable differences between the uptake values. With a 30 mass % water-containing feed mixture, the M-3 membrane exhibits a more sigmoidal trend than that of the M-1 and M-2 membranes. Surprisingly, at a 40 mass % of the water-containing mixture, the attainment of equilibrium uptake is quite fast. Thus, in general, the time required to attain equilibrium sorption decreases with an increasing amount of water in the feed mixture as well as with a decreasing amount of GG-*g*-PAAm in the blend membranes. All these data support that the blend membrane

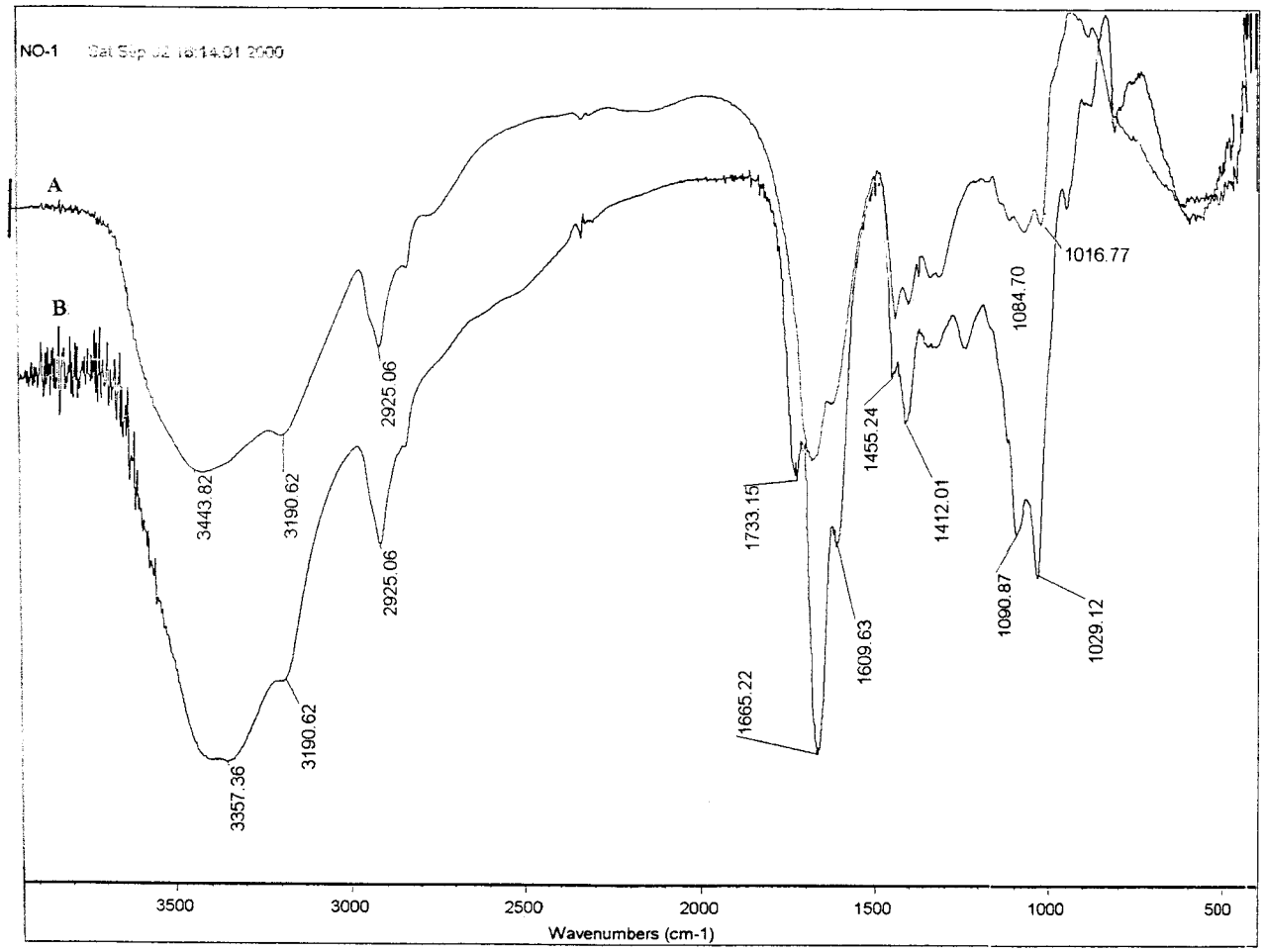

Figure 2 FTIR spectra of (A) GG-*g*-PAAm and (B) membrane M-3.

M-3 is more hydrophilic than is M-2, which, in turn, exhibits higher hydrophilicity than that of the neat Na–Alg membrane.

To find a relationship between the shapes of the sorption curves and the diffusion anomalies,

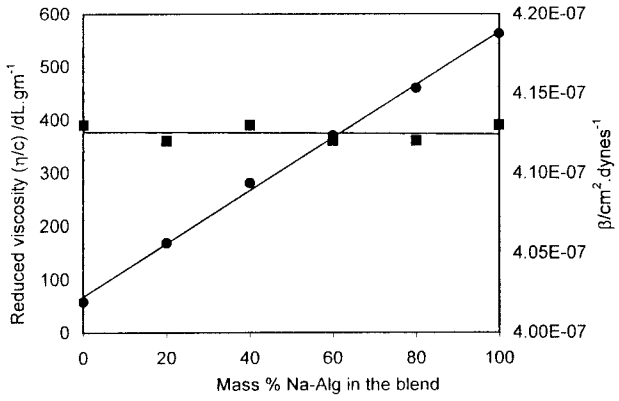

Figure 3 Variation of reduced viscosity and adiabatic compressibility with blend composition at 30°C.

we attempted to fit the experimental uptake data (i.e., M_t/M_∞) with the following empirical relation[28]:

$$\frac{M_t}{M_\infty} = kt^n \tag{11}$$

where M_∞, the equilibrium percent mass uptake of the membrane, was calculated from the asymptotic region of the curve, and k and n are the empirical parameters, of which k represents the polymer–solvent interaction, while the values of n indicate the type of transport mechanism. For the Fickian mechanism, n is around 0.5; if n varies between 0.5 and 1, then diffusion follows anomalous transport. The values of k and n were estimated by the least-squares method before 60% equilibrium. We find that the values of n vary from 0.13 to 0.98 and those of k vary from 0.027 to 0.198. However, we could not arrive at conclusive evidence of the nature of the transport phenome-

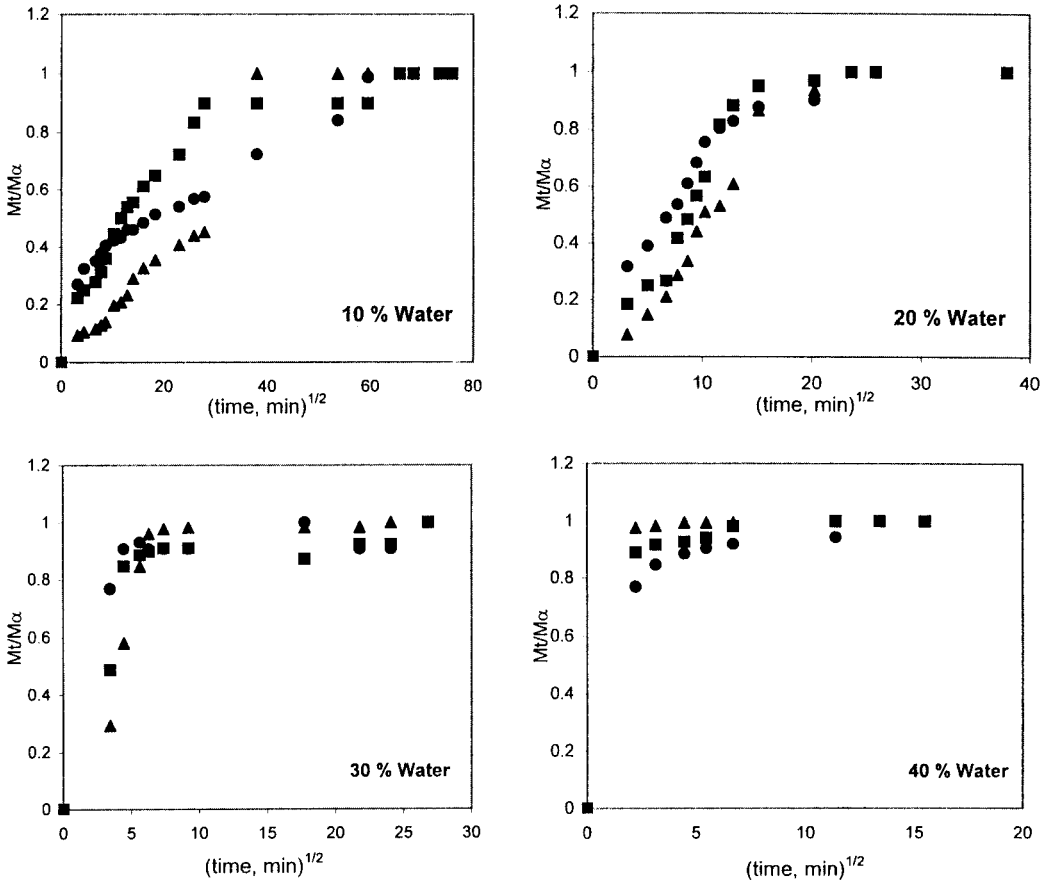

Figure 4 Variation of M_t/M_∞ versus square root of time at different mass percent of water in the feed for (●) pure sodium alginate membrane (M-1), (■) 75 : 25 blend of Na–Alg and GG-*g*-PAAm (M-2), and (▲) 50 : 50 blend of Na–Alg and GG-*g*-PAAm (M-3).

non. It appears that transport is controlled mainly by the polymer-relaxation process rather than just by the molecular phenomenon in the presence of penetrant molecules.

Equilibrium percent mass uptake at 30°C is displayed as a function of the feed water composition in Figure 5. We find that the curves exhibit sigmoidal shapes for the M-1 and M-2 membranes, signifying the presence of non-Fickian transport. However, for the M-3 membrane, equilibrium percent mass uptake exhibits the Fickian trend.

Sorption selectivity gives an indication of the membrane permseletivity and it describes how selective the membrane is toward a particular mixture component. These results for the M-1, M-2, and M-3 membranes are presented in Figure 6(A). In all cases, sorption selectivity decreases with an increasing amount of water in the feed mixture. This decrease is quite considerable at a lower water content of the feed mixture and this may be due to an insignificant swelling of the membrane. At higher amounts of water in the mixture (i.e., between 40 and 80%), sorption selectivity levels off, indicating the lesser interac-

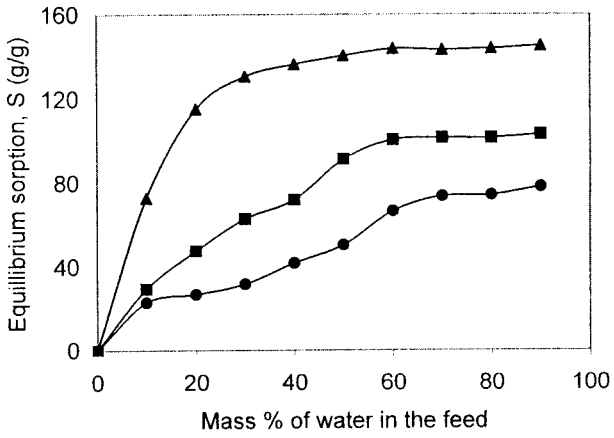

Figure 5 Variation of equilibrium percent mass uptake with mass percent of water in the feed. Symbols are the same as in Figure 4.

tion between water and the membrane material. Sorption selectivity for the pure Na–Alg membrane (M-1) is higher than that for the blend membranes.

The results of α_{sep} presented in Figure 6(B) are quite higher at 20 mass % of water for the Na–Alg membrane (M-1). This is due to a high swelling of the membrane, which selectively allows the water molecules to transport through. For the other membranes (M-2 and M-3), α_{sep} decreases with an increasing amount of water in the feed. This may be due to an increase in the free volume of the polymer, thereby facilitating the diffusion of HAc. Also, the α_{sep} values decrease with an increase in the mass percent of GG-*g*-PAAm in the blend membrane. This could possibly be due to an increase in the number of active amide groups that will significantly interact with the HAc molecules at a higher mass percent of GG-*g*-PAAm in the blend. However, in the case of M-3, the α_{sep} decreases at 30 mass % of water in the feed and then increases slightly.

The dependence of mass percent of (A) water in the permeate and (B) that of HAc in the permeate versus mass percent of water in the feed at 30°C is shown in Figure 7. It is observed that the mass percent water increases exponentially while that of HAc decreases continuously with an increasing amount of water in the feed mixture. This indicates that the membranes developed are water-selective.

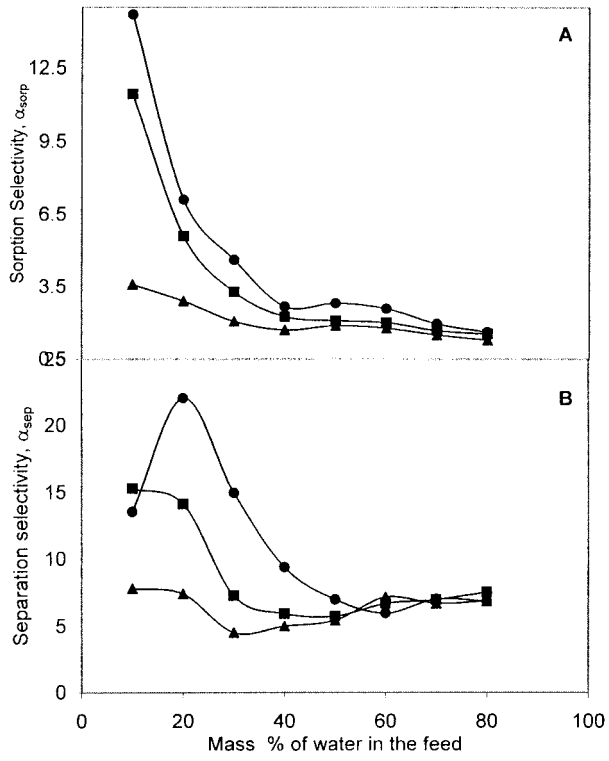

Figure 6 Variation of (A) sorption selectivity and (B) separation selectivity with mass percent of water in the feed. Symbols are the same as in Figure 4.

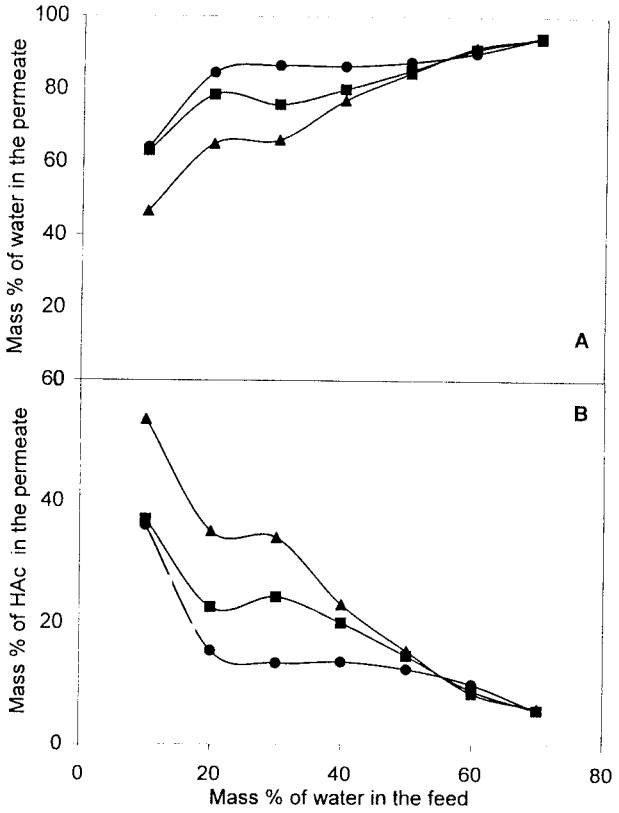

Figure 7 Variation of mass percent of (A) water and (B) HAc in the permeate mixtures with mass percent of water in the feed. Symbols are the same as in Figure 4.

PV Performance of the Membranes

Membrane performance in PV separation is influenced not only by the process parameters like feed composition and temperature, but also by the relaxation of the polymeric chains. Relaxation involves a configurational rearrangement of the polymeric chains, thereby resulting in a decrease of flux with an increase in time. However, relaxation can be complicated by the mobility of the liquid and its interaction with the polymer. A detailed analysis of the chain-relaxation process as applied to PV separation was given by Yeom et al.[29]

The permeation flux (J_p), separation selectivity (α_{sep}), permeation separation index (PSI), and

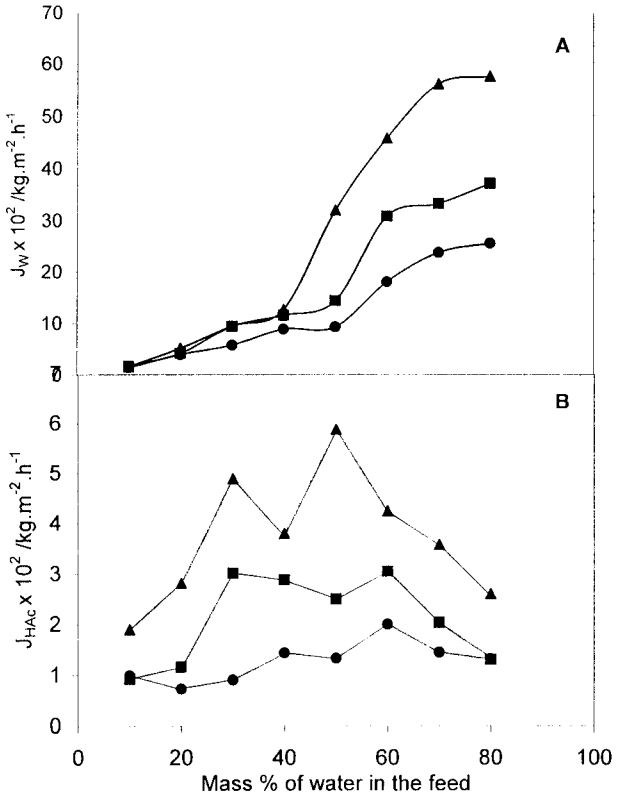

Figure 8 Variation of (A) water flux and (B) HAc flux with mass percent of water in the feed. Symbols are the same as in Figure 4.

enrichment factor (β) were calculated from eqs. (6)–(9), respectively. The results of J_p and α_{sep} are compiled in Table II. We notice that, generally, the total flux of the water + HAc mixture increases from the M-1 to M-3 membranes, and, also, with an increasing amount of water in the feed, the J_p values increase. The increase in J_P is more considerable at a higher amount of water in the feed mixture when compared to those containing a lower amount of water. The increase in J_p with an increasing amount of water in the feed mixture supports the water-selectivity of the membranes. On the other hand, α_{sep} values do not show any systematic dependence on the composition of the feed mixture, but, generally, α_{sep} decreases from the M-1 to M-3 membranes.

Flux data for water and HAc are, respectively, displayed in Figure 8(A,B). Water flux increases due to an increasing amount of water as well as an increasing amount of GG-*g*-PAAm in the blend membranes. The increase in the water flux may be due to the hydrophilicity of GG-*g*-PAAm in the blend. For all the membranes, water flux increases rapidly between 40 and 60% of water, which might be due to a change in the rubbery nature of the polymer from its originally glassy state at higher water-containing binary mixtures. However, the flux data for HAc [Fig. 8(B)] do not show any systematic dependence on the water content in the feed mixture.

A comparison of the present data with those of published reports (shown in Table IV) indicates that separation selectivity for Na–Alg and Na–Alg/GG-*g*-PAAm blend membranes are, respectively, 22.5 and 14.1 and these data are reasonably higher than for the blend membranes of PVA with other polymers as reported by Nguyen et al.[14] However, our flux values are lower by an order of magnitude than those reported by Nguyen et al., but our separation selectivity data are quite higher. With other researchers,[2,7] our results on J_p and α_{sep} are comparable. However, it may be noted that for the Nafion and TPX-*g*-PGMAS membranes, J_p and α_{sep} values are exceedingly higher than for all other membranes.[8,15]

The results of the enrichment factor, β, and the pervaporation separation index, *PSI*, are presented in the Figure 9(A,B). It is observed that the β values vary somewhat systematically with variation in the amount of water in the feed. However, no systematic variation of *PSI* in mass percent of water in the feed is observed.

Determination of Diffusion Coefficients

Transport in PV experiments has been explained by the solution–diffusion model.[30] Diffusion occurs as a result of the concentration gradient and it is important to estimate the diffusion coefficient, D_i, to understand the transport mechanism. From the PV results, we calculated D_i using the equation[8]

$$J_i = P_i[p_{i(\text{feed})} - p_{i(\text{permeate})}] = \frac{D_i}{h}[C_{i(\text{feed})} - C_{i(\text{permeate})}] \quad (12)$$

Here, D_i is assumed to be constant across the effective membrane thickness, h; $C_{i(\text{feed})}$ and $C_{i(\text{permeate})}$ are, respectively, the mixture concentrations in the feed and in the permeate. The computed values of D_i (where subscript i stands for water or HAc) at 30°C are presented in Table V. As expected, the diffusion coefficients of water increase considerably with an increasing amount of water in the feed mixture. Such an increase is

Table IV Comparison of PV Performance of Different Membranes Reported in the Literature for Water + HAc Mixtures

Membrane	Temperature (°C)	Mass % of HAc in the Feed	Flux J_p (kg m^{-2} h^{-1})	Separation Selectivity	Reference
Na–Alg (M-1)	30	80	0.047	22.5	Present work
Na–Alg/GG-*g*-PAAm (M-2)	30	80	0.054	14.1	Present work
Na–Alg/GG-*g*-PAAm (M-3)	30	80	0.080	7.4	Present work
Composite membrane of Na–Alg and PAN crosslinked with HDM	40	90	0.037	38.0	7
Composite membrane of Na–Alg and PAN crosslinked with PVA	50	90	0.094	18.0	7
PVA-*g*-PAAm (poly 1)	35	80	0.056	3.9	2
PVA/PAA (blend membranes)	25	90	0.300	6.6	14
PVA/PHC	25	90	0.140	7.9	14
PVA/PVP	25	90	0.800	2.4	14
PVA	25	90	0.500	4.5	14
TPX-*g*-PGMAS with 13.7% degree of grafting	35	84	0.073	125.0	15
Nafion $(C_8H_{17})_4N^+$	25	90	0.180	243.0	8

Na–Alg, sodium alginate; PAAm, poly(acryl amide); PAN, polyacrylonitrile; PVA, poly(vinyl alcohol); PAA, poly(acrylic acid); PHC, poly(hydroxycarboxylic acid); PVP, poly(*N*-vinyl-2-pyrolidone); HDM, 1,6-hexanediamine; TPX, poly(4-methyl-1-pentene); PGMAS, poly(glycidyl methacrylate sulfonic acid).

quite dramatic at higher compositions of water in the feed. Even though similar trends are observed for HAc, the D_i values of HAc do not vary systematically with the composition of water in the feed mixture. Such an increase in D_i with an increasing amount of water in the feed mixture is attributed to the creation of extra free volume in the membrane matrix. As regards the nature of the membranes, diffusion coefficients increase with an increasing amount of GG-*g*-PAAm in the blend membrane, that is, D_i values of both water and HAc increase systematically from M-1 to M-3. This dependence is similar to the permeation flux values discussed before. It may be noted that D_i values calculated from eq. (12) are about two orders of magnitude higher than are those computed from eq. (4). This difference is attributed to the nature of different types of transport processes from which the diffusion coefficients were calculated.

Effect of Temperature

Table III presents the results of PV flux and separation selectivity at 30, 40, and 50°C. It is observed that the flux values increase systematically with increasing temperature, whereas separation selectivity values decrease with increasing temperature. The temperature dependency of the permeation flux was studied by the Arrhenius relationship:

$$J_P = J_{P0}\exp(-E_P/RT) \tag{13}$$

where E_P is activation energy for permeation; J_{P0}, the permeation rate constant; R, the gas constant; and T, the temperature in Kelvin. If the activation energy is positive, then permeation flux increases with increasing temperature and this has been observed in most PV experiments.[31,32] Apart from the enhanced liquid permeation flux, the driving force for mass transport also increases with increasing temperature. This driving force represents the concentration gradient resulting from a difference in partial vapor pressure of the permeants between the feed and the permeate. As the feed temperature increases, vapor pressure in the feed compartment also increases, but vapor pressure at the permeate side

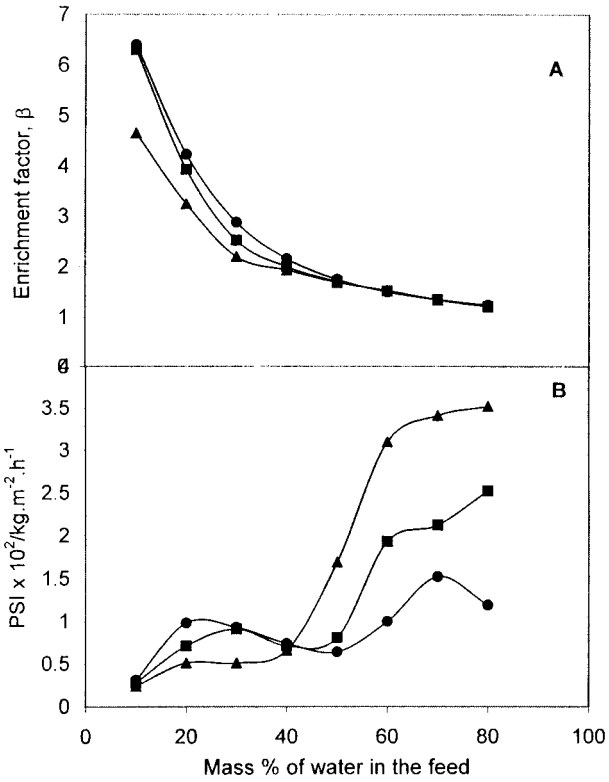

Figure 9 Variation of (A) enrichment factor and (B) permeation separation index with mass percent of water in the feed. Symbols are the same as in Figure 4.

is not affected. This results in an increase of driving force with an increase in temperature.

Arrhenius plots of log J_P versus 1000/T shown in Figure 10 represents the temperature dependence of the total permeation flux. In all cases, linear behavior is observed, signifying that the temperature dependence of total permeation flux or diffusivity follows the Arrhenius trend. The apparent activation energy values (E_P and E_D for permeation and diffusion, respectively) calculated from the slopes of the straight lines of the Arrhenius plots by the least-squares method are presented in Table VI. The E_P values show a decreasing tendency from M-1 to M-3.

In a similar manner, the mass transport is secured by an activated diffusion given by the Arrhenius equation:

$$D_i = D_{i0}\exp(-E_D/RT) \tag{14}$$

where E_D is energy of activation for diffusion and i stands for water or HAc. The Arrhenius plots of log D_i versus 1000/T are shown in Figure 11(A,B) for water and for HAc, respectively. The E_D values estimated by the method of least squares included in Table VI are higher for M-1 than for the M-2 and M-3 membranes. The calculated values of the heat of sorption, $\Delta H_S(\cong E_P - E_D)$ are also included in Table VI. The ΔH_S values are negative in all the cases, suggesting an endothermic mode of sorption.

The temperature dependence of α_{sep} was further studied by employing the relationship proposed earlier by Ping et al.[33]:

$$Y_w = \frac{1}{1 + (J_{HAc}/J_W)\exp(-(E_{HAc} + E_W)/RT)} \tag{15}$$

where Y_w is water composition in the permeate; J_W and J_{HAc}, the permeation fluxes; and E_W and E_{HAc}, the Arrhenius activation energies of water and HAc, respectively, at the average energy level. A positive value of $[E_{HAc} - E_W]$ indicates that the α_{sep} decreases with increase in the temperature and the negative value indicates that α_{sep} increases with increase in the temperature.[30] In all the present membranes, these values are

Table V Diffusion Coefficients of Water and HAc Calculated from Eq. (12) at 30°C

Mass % of Water in the Feed	$D_w \times 10^{10}$ (m²/s)			$D_{HAc} \times 10^{10}$ (m²/s)		
	M-1	M-2	M-3	M-1	M-2	M-3
10	6.9	8.0	11.3	4.60	4.6	13.0
20	15.3	18.0	28.9	2.80	5.0	15.6
30	25.6	51.3	66.0	4.00	16.4	34.0
40	47.8	72.0	85.8	7.60	18.0	25.6
50	62.1	102	233	8.80	17.8	42.6
60	92.5	249	363	16.6	24.6	33.8
70	245	344	585	15.0	20.9	37.4
80	383	538	873	19.7	19.7	31.5

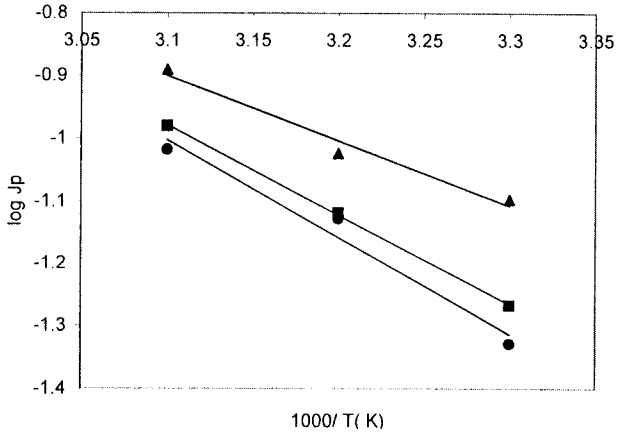

Figure 10 Variation of log J_p with 1000/T at 20 mass % of water in the feed. Symbols are the same as in Figure 4.

positive (see Table VI), further supporting that α_{sep} decreases with increasing temperature. Contrary to this, selectivity decreases with increasing temperature from 30 to 40°C, but not much difference in the α_{sep} values is observed between 40 and 50°C (see Table III).

Conclusions

Pure sodium alginate and blend membranes of sodium alginate with GG-*g*-PAAm were used for the separation of HAc and water mixtures. The permeation flux of the membranes showed an increase with an increasing amount of GG-*g*-PAAm in the blend, while the separation selectivity decreased. Increase in the flux was due to an enhanced hydrophilicity and, hence, an augmented free volume of the matrix. Decreased selectivity could be the result of increased —NH_2 groups in the membrane, which interact strongly with the —COOH group of HAc. The PV results reported in this study are comparable and, in some cases, better than those for other membranes reported in the literature. However, more research is needed to optimize the separation characteristics of these membranes for other aqueous–organic mixtures. Work in this area is under progress in our laboratory.

Table VI Permeation and Diffusion Activation Energies, Heat of Sorption for Water, and Energy-difference Values

Parameter	M-1	M-2	M-3
E_P (kJ/mol) eq. (13)	29.02	26.93	19.30
E_D (kJ/mol) eq. (14)	29.88	28.57	24.08
ΔH_S (kJ/mol)	−0.86	−1.64	−4.78
$E_{HAc} - E_W$ (kJ/mol) eq. (15)	8.76	16.34	22.17

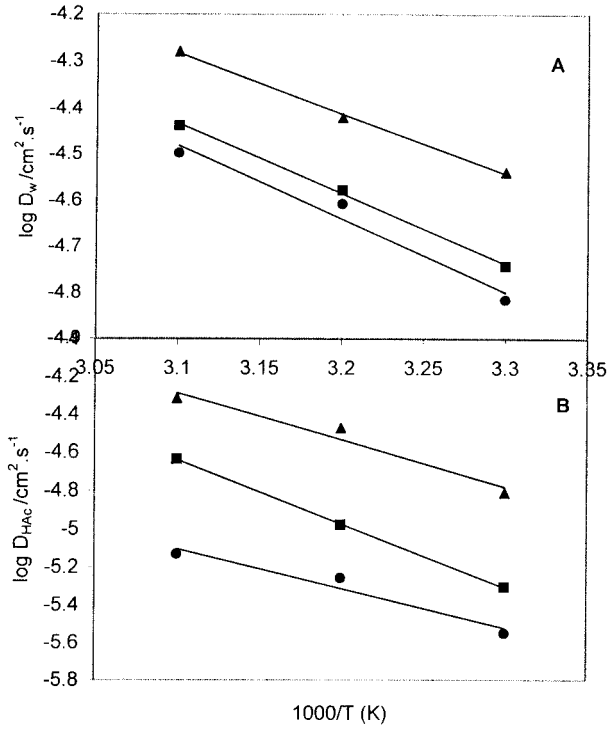

Figure 11 Variation of (A) log D_w and (B) log D_{HAc} with 1000/T at 20 mass % of water in the feed. Symbols are the same as in Figure 4.

We thank the Department of Science and Technology, New Delhi [Grant No. SP/S1/H-26/96 (PRU)] for financial support of this research program.

REFERENCES

1. Aminabhavi, T. M.; Khinnavar, R. S.; Harogoppad, S. B.; Aithal, U. S.; Nguyen, Q. T.; Hansen, K. C. J Macromol Sci-Rev Macromol Chem Phys C 1994, 43, 139.
2. Aminabhavi, T. M.; Naik, H. G. J Appl Polym Sci 2002, 83, 244.
3. Moon, G. Y.; Pal, R.; Huang, R. Y. M. J Membr Sci 1999, 156, 17.
4. Yoem, C. K.; Lee, K. H. J Appl Polym Sci 1998, 67, 949.
5. Huang, R. Y. M.; Pal, R.; Moon, G. Y. J Membr Sci 1998, 160, 101.
6. Kirk–Othmer Encyclopedia of Chemical Technology, 3rd ed.; Grayson, M., Ed.; Wiley: New York, 1978; Vol. 1.

7. Wang, X. P. J Membr Sci 2000, 170, 71.
8. Kusumocahyo, S. P.; Sudoh, M. J Membr Sci 1999, 161, 77.
9. Ray, S. K.; Sawant, S. B.; Joshi, J. B.; Pangarker, V. G. J Membr Sci 1998, 138, 1.
10. Lee, Y. M.; Oh, B. K. J Membr Sci 1993, 85, 13.
11. Kusumocahyo, S. P.; Sano, K.; Sudoh, M.; Kensaka, M. Sep Purif Technol 2000, 18, 141.
12. Huang, R. Y. M.; Rhim, J. W. Polym Int 1993, 30, 129.
13. Huang, R. Y. M.; Yeom, C. K. J Membr Sci 1991, 62, 59.
14. Nguyen, Q.; Essamri, T.; Clement, A.; Nee, R. J Makromol Chem 1987, 188, 1973.
15. Lee, J.; Wang, F. Y. C. Sep Sci Technol 1998, 33, 187.
16. Yoshikawa, M. Y.; Kuno, S. I.; Kitao, T. J Appl Polym Sci 1994, 51, 1021.
17. Bai, J.; Fouda, A. E.; Matsuura, T.; Hazlett, J. D. J Appl Polym Sci 1993, 48, 999.
18. Soppimath, K. S.; Kulkarni, A. R.; Aminabhavi, T. M. Int Symp Control Rel Bioact Mater 2000, 27, 847.
19. Aminabhavi, T. M.; Banerjee, K. J Chem Eng Data 1998, 43, 852.
20. Toti, U. S.; Kariduraganavar, M. Y.; Aralaguppi, M. I.; Aminabhavi, T. M. J Chem Eng Data, in press.
21. Aralaguppi, M. I.; Aminabhavi, T. M.; Balundgi, R. H.; Joshi, S. S. J Phys Chem 1991, 95, 5299.
22. Aminabhavi, T. M.; Phayde, H. T. S.; Ortego, J. D.; Vergnaud, J. M. Polymer 1996, 37, 1677.
23. Owen, D. R.; Shen, T. C. In Structure Solubility Relationship in Polymers; Harries, F. W.; Seymour, R. B., Eds.; Academic: New York, 1977.
24. Rao, V.; Ashokan, P. V.; Shridhar, M. H. Polymer 1999, 40, 7167.
25. Yeom, C. K.; Lee, K. H. J Appl Polym Sci 1998, 67, 209.
26. Mulder, M. H. V.; Smolders, C. A. J Membr Sci 1984, 17, 289.
27. Kim, H. Y.; Jo, W. H.; Kang, Y. S. J Appl Polym Sci 1995, 57, 63.
28. Peppas, N. A. Pharm Acta Helv 1985, 60, 110.
29. Yeom, C. K.; Jegal, J. G.; Lee, K. H. J Appl Polym Sci 1996, 62, 1561.
30. Binning, R. C.; Lee, R. J.; Jennings, J. F.; Martin, E. C. Ind Eng Chem 1961, 53, 45.
31. Burshe, M. C.; Netke, S. A.; Sawant, S. B.; Joshi, J. B.; Pangarkar, V. G. Sep Sci Technol 1997, 32, 1335.
32. Nam, S. Y.; Lee, Y. M. J Membr Sci 1999, 157, 63.
33. Ping, Z. H.; Nguyen, Q. T.; Clement, R.; Neel, J. J Membr Sci 1990, 48, 297.